Inorganic Chemistry

ARTICLE

pubs.acs.org/IC

Alkali-Metal-Supported Bismuth Polyhedra—Principles and Theoretical Studies

Kirill Yu. Monakhov,[†,§] Gerald Linti,[*,†] Lando P. Wolters,[‡] and F. Matthias Bickelhaupt[*,‡]

[†]Anorganisch-Chemisches Institut, Universität Heidelberg, Im Neuenheimer Feld 270, D-69120 Heidelberg, Germany

[‡]Department of Theoretical Chemistry and Amsterdam Center for Multiscale Modeling, VU University Amsterdam, De Boelelaan 1083, NL-1081 HV, Amsterdam, The Netherlands,

Supporting Information

ABSTRACT: We have quantum chemically investigated the structure, stability, and bonding mechanism in highly aggregated alkali-metal salts of bismuthanediide anions $[RBi]^{2-}$ using relativistic density functional theory (DFT, at ZORA-BP86/TZ2P) in combination with a quantitative energy decomposition analysis (EDA). Our model systems are alkali-metal-supported bismuth polyhedra $[(RBi)_nM_{2n-4}]^{4-}$ with unique interpenetrating shells of a bismuth polyhedron and an alkali-metal superpolyhedron. Furthermore, we have analyzed the trianionic inclusion complexes $[M'@\{(RBi)_nM_{2n-4}\}]^{3-}$ involving an additional endohedral alkali-metal ion M′. The main objective is to assist the further development of synthetic approaches toward this class of compounds. Our analyses led to electron-counting rules relating, for example, the number of bonding orbitals (N_{bond}) of the cage molecules $[(RBi)_nM_{2n+Q}]^{Q}$ to the number of bismuth atoms (n_{Bi}), alkali-metal atoms (n_M), and net charge Q as $N_{bond} = n_{Bi} + n_M - Q$ (R = one-electron donor ligand; M = alkali metal; $n = 4-12$; $Q = -4, -6, -8$). Finally, on the basis of our findings, we predict the next members in the 5-fold symmetrical row of alkali-metallobismaspheres with a macroicosahedral arrangement.

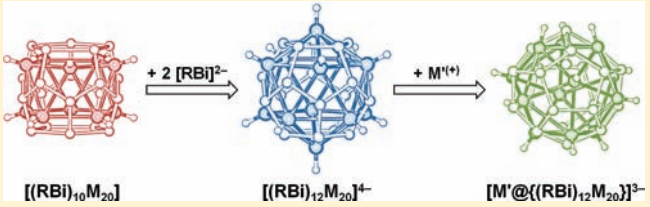

INTRODUCTION

The beauty of the structural chemistry of the heavier group 15 elements reveals itself in their ligator-stabilized polyhedra, namely alkali-metal pnictodiides, which form highly aggregated structures ligated by alkali-metal ions. These compounds are of relevance for molecular clustering and self-assembly. Not only the beauty of this young class of compounds attracts significant attention, but the chemistry of "elementanediides" $[RE]^{2-}$ opens a novel field for the group 15 elements. These aggregate with alkali-metal ions to cage molecules, whose size and structure might be influenced by the substituents and the size of the metal ion. Furthermore, these unique multiple-shell compounds are excellent container molecules[1,2] with structural principles related to the ones for polyoxometalates.[1,3] Their capability to trap ions and small molecules is comparable to that of fullerene spheres.[4] The building units $[RE]^{2-}$ might be valuable reagents for synthesis of cyclic and polymeric bismuth compounds.

The development of synthetic methods toward metalated $MBiR_2$[2,5] and M_2BiR species constitutes one of the grand challenges in bismuth chemistry. This contrasts with the situation for MER_2 and M_2ER compounds of phosphorus and arsenic (E = P, As) for which synthetic routes are readily available and which have already a well-developed chemistry (they are, for example, among the most reactive nucleophilic transfer reagents). The lack of stable hydrogen compounds of bismuth has led to a low interest in metalated bismuthines.[6] Only in 2000, Power et al. reported the first stable diarylbismuthine.[7] The simple metalated species such as $MBiR_2$ and M_2BiR could serve as versatile templates for manipulations on their insertion as transfer reagents in inorganic and organometallic metathesis reactions and open a wide range for the metal−metal interactions.

As was remarked by Driess, the tendency of dimetalated phosphanes and arsanes M_2ER "to aggregate" is intermediate compared to molecular MER_2 and ionic M_3E species (E = P, As).[1] Thus, the structural chemistry of doubly metalated M_2PR and M_2AsR revealed a high diversity of cluster shapes (octameric, decameric, and dodecameric), polynuclearity, and the presence of a variety of internal inclusions (filled cages) as well as their absence ("empty" cages). The most interesting here are pseudoicosahedral frameworks $(RP)_{12}Li_{20}$ and $(RAs)_{12}M_{20}$ (M = Li, Na) with an interstitial group of "guest" atoms, namely, M_nO-filled cages (Scheme 1).[1]

In most cases, M_nO (M = Li, Na; n = 2, 6) units are accommodated in the voids, namely, in the center of the spherical molecules, and have close contacts with the walls of the cages. All of the observed "host−guest complexes" of P and As of above type known up to now are neutral at the expense of compensation of their charge by interstitial countercations (filled-cages) and/or mixed valence of pnictogen ("empty" cages); i.e., they do not have external counterions.

Received: March 23, 2011
Published: May 25, 2011

Scheme 1. Topological Representation of Driess's Clusters $(RE)_{12}M_{20}$ (E = P, As; M = Li, Na) with an Endohedral Inclusion of "Guest" Atoms, Namely, M_nO-Filled Cages[a]

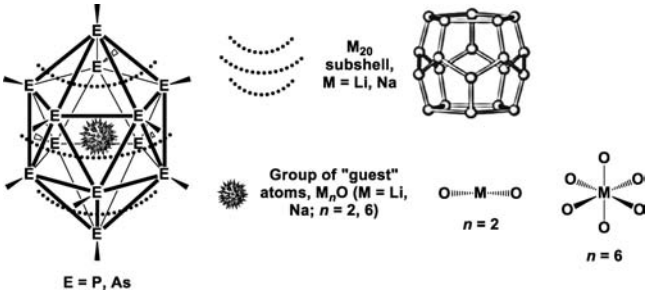

[a] See ref 1 and references cited therein.

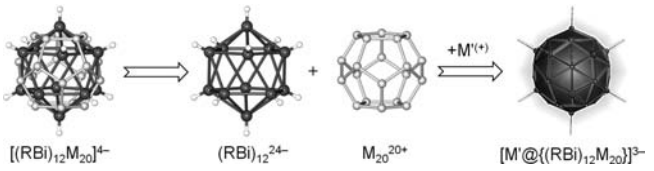

Figure 1. Topological decomposition of nonfilled ("empty") structure of a highly aggregated alkali-metal salt of bismuthanediide $[RBi]^{2-}$ ions, namely, $[(RBi)_{12}M_{20}]^{4-}$, where the icosahedral $(BiR)_{12}^{24-}$ subunit is capped by an alkali-metal subshell ("the ligator atoms", M_{20}^{20+}) in pentagonal dodecahedral arrangement.

The first and sole, up to now, observation of a polymetalated bismuthanide polyanionic system, $[Na'@\{(t\text{-}Bu_3Si)_{12}Bi_{12}Na_{20}\}]^{3-}$, was reported in 2002.[2] The observed architecture is a balllike cage, consisting of a Bi_{12} icosahedron covered by lipophilic bulky t-Bu_3Si groups and face-capped by 20 sodium atoms (Figure 1). The architecture contains one encapsulated sodium atom in a disordered position that partially compensates the 4-fold negative charge of the $[(t\text{-}Bu_3Si)_{12}Bi_{12}Na_{20}]^{4-}$ cage. $[Na(thf)_6]^+$ and two $[Na(thf)_4]^+$ molecules act as counterions. The molecular assembly has been observed as one of the reaction products in the conversion of $BiBr_3$ with bulky sodium silanide $Na(thf)_2(t\text{-}Bu_3Si)$.

The unique arrangement of the $[Na'@\{(t\text{-}Bu_3Si)_{12}Bi_{12}Na_{20}\}]^{3-}$ salt prompted us to undertake the first comprehensive computational study of dimetalated and polymetalated bismuth compounds, using relativistic, gradient-corrected density functional theory as implemented in the ADF program.[8] Our objectives are manifold. In the first place, we wish to obtain a better understanding of the precise equilibrium structure of the empty cage, as well to develop electron-counting rules for skeletal electron bookkeeping of the empty *closo-, nido-, and arachno*-cage molecules with different stoichiometric ratios of substituents (at Bi), bismuth atoms, and alkali metals. Second, we have determined the stability of binding an endohedral alkali cation. In order to put our results into broader context, we have explored model systems beyond the lithium and sodium species, involving heavier alkali metals, such as K, Rb, and Cs. On the basis of molecular modeling, electronic structure calculations, and energy decomposition analyses, we have got an insight into the arrangement, stability, and nature, as well perspectives on the further employment of the empty icosahedral cages and their endohedral derivatives with different alkali-metal subshells. The main goal of our investigations is to develop structural principles and efficient synthetic approaches to the above-mentioned molecules.

METHODS AND THEORY

Computational Details. All calculations were performed using the Amsterdam density functional (ADF) program developed by Baerends and others.[8,9] The numerical integration was performed using the procedure developed by te Velde et al.[9g,h] The MOs were expanded in a large uncontracted set of Slater-type orbitals (STOs) containing diffuse functions: TZ2P (no Gaussian functions are involved).[9i] The basis set is of triple-ζ quality for all atoms and has been augmented with two sets of polarization functions, i.e., 2p and 3d on H, and d and f on Li, Na, K, Rb, Cs, and Bi. Moreover, an extra set of p functions has been added to the basis sets of the alkali metals. The core shells of Li and Na (1s), K (1s2s), Rb (up to 3p), Cs (up to 3d), and Bi (up to 4d) were treated by the frozen-core approximation.[9c] An auxiliary set of s, p, d, f, and g STOs was used to fit the molecular density and to represent the Coulomb and exchange potentials accurately in each self-consistent field cycle.[9j]

Equilibrium structures were optimized using analytical gradient techniques.[9k] Geometries and energies were calculated at the BP86 level of the generalized gradient approximation (GGA): exchange is described by Slater's Xα potential[9l] with nonlocal corrections due to Becke[9m,n] added self-consistently and correlation is treated in the Vosko–Wilk–Nusair (VWN) parametrization[9o] with nonlocal corrections due to Perdew[9p] added, again, self-consistently (BP86).[9q] Energy minima in the gas phase have been verified to be equilibrium structures through vibrational analysis.[10] All minima were found to have zero imaginary frequencies. Scalar relativistic effects were accounted for using the zeroth-order regular approximation (ZORA).[11]

Bond Analysis. To obtain a deeper insight into the stability and the nature of internal interactions and bonding in trianionic endohedral frameworks, an energy decomposition analysis (EDA) has been carried out.[12−14] In this analysis, the total binding energy ΔE associated with forming a molecular structure from smaller molecular fragments, say, A and B, is in general made up of two major components (eq 1):

$$\Delta E = \Delta E_{prep} + \Delta E_{int} \quad (1)$$

In this formula, the preparation energy (ΔE_{prep}) is the amount of energy required to deform two individual (isolated) fragments A and B from their equilibrium structure to the geometry that they acquire in the overall molecule. The interaction energy (ΔE_{int}) corresponds to the actual energy change when these geometrically deformed fragments are combined to form the overall molecule. It is analyzed in the framework of the Kohn–Sham molecular orbital (MO) model[12−15] using a quantitative decomposition into electrostatic interaction, Pauli repulsion (or exchange repulsion or overlap repulsion), and (attractive) orbital interactions (eq 2).[12]

$$\Delta E_{int} = \Delta V_{elstat} + \Delta E_{Pauli} + \Delta E_{oi} \quad (2)$$

The term ΔV_{elstat} corresponds to the classical electrostatic interaction between the unperturbed charge distributions ρ_A and ρ_B of the prepared (i.e., deformed) fragments that adopt their positions in the overall molecule and is usually attractive. The Pauli repulsion term (ΔE_{Pauli}) comprises the destabilizing interactions between occupied orbitals and is responsible for the steric repulsion. This repulsion is caused by the fact that two electrons with the same spin cannot occupy the same region in space. It arises as the energy change associated with the transition from the superposition of the unperturbed electron densities $\rho_A + \rho_B$ of the geometrically deformed fragments to the wave function $\psi^0 = N\hat{A}[\psi_A\psi_B]$, which properly obeys the Pauli principle through explicit antisymmetrization ($\hat{A}$ operator) and renormalization (N constant) of the product of fragment wave functions. The orbital interaction (ΔE_{oi}) in any MO model, and therefore also in Kohn–Sham theory, accounts for electron-pair bonding,[12] charge transfer (i.e., donor–acceptor interactions between occupied orbitals on one moiety with unoccupied orbitals of the other, including the HOMO–LUMO interactions), and polarization (empty–occupied orbital mixing on one fragment due to the presence of another fragment).

Table 1. Link between the Families of the Bare Bismuth Cluster Polycations and the Salts of Alkali-Polymetalated Bismuthanediide Anions

polycationic cluster with $n = 4-12$	number of bonding orbitals	number of bonding electrons	salt polyanions with $n = 4-12$	number of bonding orbitals	number of bonding electrons
closo-$Bi_n^{(n-2)+}$	$n + 1$	$2n + 2$	*closo*-$[(RBi)_nM_{2n-4}]^{4-}$	$n_{Bi} + n_M + 4$	$2(n_{Bi} + n_M) + 8$
nido-$Bi_n^{(n-4)+}$	$n + 2$	$2n + 4$	*nido*-$[(RBi)_nM_{2n-6}]^{6-}$	$n_{Bi} + n_M + 6$	$2(n_{Bi} + n_M) + 12$
arachno-$Bi_n^{(n-6)+}$	$n + 3$	$2n + 6$	*arachno*-$[(RBi)_nM_{2n-8}]^{8-}$	$n_{Bi} + n_M + 8$	$2(n_{Bi} + n_M) + 16$

The orbital interaction energy can be decomposed into the contributions from each irreducible representation Γ of the interacting system (eq 3) using the extended transition state (ETS) scheme developed by Ziegler and Rauk[13] (note that our approach differs in this respect from the Morokuma scheme,[14] which instead attempts a decomposition of the orbital interactions into polarization and charge transfer).

$$\Delta E_{oi} = \sum_{\Gamma} \Delta E_{\Gamma} \qquad (3)$$

Charge Analysis. The electron density distribution is analyzed using the Voronoi deformation density (VDD) method[16] and the Hirshfeld scheme[17] for computing atomic charges. The VDD atomic charge Q_A^{VDD} is computed as the (numerical) integral[9a,g,h] of the deformation density $\Delta\rho(\mathbf{r}) = \rho(\mathbf{r}) - \Sigma_B\rho_B(\mathbf{r})$ in the volume of the Voronoi cell of atom A (eq 4). The Voronoi cell of atom A is defined as the compartment of space bounded by the bond midplanes on and perpendicular to all bond axes between nucleus A and its neighboring nuclei (cf. the Wigner−Seitz cells in crystals[16c]).

$$Q_A^{VDD} = -\int_{\text{Voronoi cell of A}} \left(\rho(\mathbf{r}) - \sum_B \rho_B(\mathbf{r})\right) d\mathbf{r} \qquad (4)$$

Here, $\rho(\mathbf{r})$ is the electron density of the molecule and $\Sigma_B\rho_B(\mathbf{r})$ the superposition of atomic densities ρ_B of a fictitious promolecule without chemical interactions that is associated with the situation in which all atoms are neutral. The interpretation of the VDD charge Q_A^{VDD} is rather straightforward and transparent. Instead of measuring the amount of charge associated with a particular atom A, Q_A^{VDD} directly monitors how much charge flows, due to chemical interactions, out of ($Q_A^{VDD} > 0$) or into ($Q_A^{VDD} < 0$) the Voronoi cell of atom A, that is, the region of space that is closer to nucleus A than to any other nucleus.

RESULTS AND DISCUSSION

Skeletal Electron Bookkeeping. The Wade−Williams−Rudolph rules[18] allow one to predict structures of polyhedral clusters on basis of their number of skeletal electron pairs (N_{SEP}). Thus, bismuth cluster polycations, which could be isolated in intermetallic phases (some bismuth polycations such as Bi_5^{3+}, Bi_5^{+}, Bi_6^{2+}, Bi_8^{2+}, Bi_9^{5+}, and Bi_{10}^{4+} are already experimentally observed),[19] have structures conforming to those rules. Their molecular forms $(RBi)_n^{2n-}$ stabilized by the alkali-metal ligator atoms (M_{2n+Q}) need adapted counting rules (Table 1). Alkali-metal bismuthanediide cages can be considered as ionic aggregates. Nevertheless, electron bookkeeping for $[(RBi)_nM_{2n+Q}]^{Q}$ (R, one-electron donor ligand; M, alkali metal; Q, net charge of the molecule) leads to the $N_{bond} = n_{Bi} + n_M - Q$ bonding orbitals rules (N_{bond}, number of bonding orbitals; n_{Bi}, number of bismuth atoms; n_M, number of alkali-metal atoms; Q, net charge) for three types of polyhedra (Table 1):

(i) $[(n_{Bi} + n_M) + 4]$ bonding orbitals with $[2(n_{Bi} + n_M) + 8]$ bonding electrons for *closo*-$[(RBi)_nM_{2n-4}]^{4-}$,

(ii) $[(n_{Bi} + n_M) + 6]$ bonding orbitals with $[2(n_{Bi} + n_M) + 12]$ bonding electrons for *nido*-$[(RBi)_nM_{2n-6}]^{6-}$,

(iii) $[(n_{Bi} + n_M) + 8]$ bonding orbitals with $[2(n_{Bi} + n_M) + 16]$ bonding electrons for *arachno*-$[(RBi)_nM_{2n-8}]^{8-}$.

This allows us to connect the stoichiometry. Scheme 2 represents the shapes of some bare bismuth polycations systematized by *closo-, nido-, and arachno*-geometry principles to give above stoichiometric ratios of highly aggregated salts by alkali-metal capping of bismuth polyhedral faces.

Scheme 2. Shapes of Some Bare Bismuth Cluster Polyions with Polyhedral Faces Available for Capping by Alkali-Metal Atoms[a]

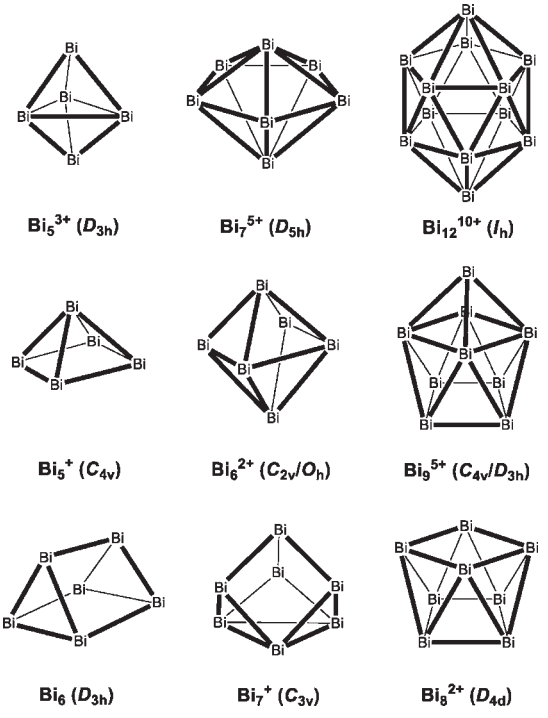

[a] First row: *closo*-$Bi_n^{(n-2)+}$.[19,20] Second row: *nido*-$Bi_n^{(n-4)+}$ (Bi_6^{2+} and Bi_9^{5+} symmetry presented as calcd/exptl).[19,20] Third row: *arachno*-$Bi_n^{(n-6)+}$.[19,20]

We propose that the stability and thus feasibility of these frameworks increase as the net charge decreases, i.e., in the order *arachno*-$[(RBi)_nM_{2n-8}]^{8-}$ < *nido*-$[(RBi)_nM_{2n-6}]^{6-}$ < *closo*-$[(RBi)_nM_{2n-4}]^{4-}$. We also predict that an increase in polynuclearity of the tetraanion cage will increase kinetic stability of the ionic cage compounds, due to a more diffuse distribution of the net charge.

On the basis of our conclusions as well the experimental findings we computationally study in the following only *closo*-$[(RBi)_nM_{2n-4}]^{4-}$ ions and their derivatives, where R substituents

dx.doi.org/10.1021/ic200596c |*Inorg. Chem.* 2011, 50, 5755–5762

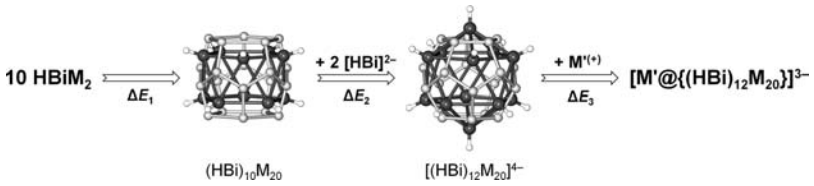

Figure 2. Topological representation of the process steps rationalized in the theoretical approach to forming 5-fold symmetrical structures, $(HBi)_{10}M_{20}$ and $[(HBi)_{12}M_{20}]^{4-}$ (M = Li, Na, K, Rb, Cs), and to encapsulating an alkali-metal ion $M'^{(+)}$ inside $[(HBi)_{12}M_{20}]^{4-}$ cages, leading to the formation of low symmetrical, endohedral alkali-metallobismaspheres $[M'@\{(HBi)_{12}M_{20}\}]^{3-}$, where $M'^{(+)} = Li^+, Na^+, K^+, Rb^+, Cs^+$.

were simplified to hydrogen; as M we have employed Li, Na, K, Rb, and Cs, and Bi_n corresponds to a Bi_{12} subunit.

Finally, we point out a very intriguing relationship between the class of the empty spheres *closo*-$[(RBi)_nM_{2n-4}]^{4-}$ and the cubane-like hybrid Zintl metal carbonyl cluster $[Bi_4\{\mu_3\text{-}Fe(CO)_3\}_4\{\mu_1\text{-}Fe(CO)_4\}_4]^{4-}$.[21] Both of these heterometallic system compounds have non-Wade's structures and stoichiometric ratios, namely, $[(RBi)_nM_{2n-4}]^{4-}$ and $[(LBi)_nL'_{2n-4}]^{4-}$, where $L = Fe(CO)_4$ and $L' = Fe(CO)_3$.

General Approach. To conceptualize the theoretical constructs and to achieve the required goals and results, we have applied a "step-by-step approach" by starting from the small alkali-dimetalated bismuthanediides $HBiM_2$ via pentagonal antiprisms $(HBi)_{10}M_{20}$ toward the nonfilled ("empty") icosahedral $[(HBi)_{12}M_{20}]^{4-}$ (see Figure 1) and their endohedral $[M'@\{(HBi)_{12}M_{20}\}]^{3-}$ frameworks, where M, M′ = Li, Na, K, Rb, or Cs (Figure 2). To better understand the anatomy of these complicated systems, we have employed a multiple shell description suggested by Driess, which is based on a topological description of interpenetrating subshells with a close packing.[1] The obtained results have revealed very interesting behavior of the cage molecules.

(Pseudo)Icosahedral Frameworks. *A. Geometric Properties.* The $HBiM_2$ molecules, which were used as templates to build double "open-faced" $(HBi)_{10}M_{20}$ frameworks, display C_s symmetry with the exception of the dilithiated one, $HBiLi_2$, which adopts a C_1-symmetric equilibrium structure. The $HBiM_2$ monomers feature essentially nonbonding M−M distances if compared to M_2 molecules. In noncharged $(RBi)_{10}M_{20}$ molecules, the M−M distances cover a broad range, but the shortest ones are comparable (M = Li, Na, K) or even shorter (M = Rb, Cs) than in M_2. The oligomerization of 10 $HBiM_2$ molecules to give $(HBi)_{10}M_{20}$ frameworks leads to a significant elongation of the Bi−M bond lengths. This trend increases from lithium to cesium cages (see Supporting Information Table S1).

The empty icosahedral $[(HBi)_{12}M_{20}]^{4-}$ structures were constructed from the $(HBi)_{10}M_{20}$ units and two bismuthanediide anions, $[HBi]^{2-}$ (Figure 2). In the case of the heavier alkali-metal ions, the Bi−Bi distances moderately increase as $(HBi)_{10}M_{20}$ structures are capped by two $[HBi]^{2-}$ ions to yield $[(HBi)_{12}M_{20}]^{4-}$ frameworks. This elongation increases from sodium to cesium. The Bi−M bond lengths in $[(HBi)_{12}M_{20}]^{4-}$ are elongated in comparison to those in $(HBi)_{10}M_{20}$. Furthermore, they become practically identical to the longest Bi−M bond lengths in the latter. The M−M separations in $[(HBi)_{12}M_{20}]^{4-}$ are all almost equal and within the range of the M−M separations in the $(HBi)_{10}M_{20}$ structures (see Supporting Information Table S1).

The encapsulation of any alkali-metal ion $M'^{(+)}$ into the 5-fold symmetrical $[(HBi)_{12}M_{20}]^{4-}$ lowers the symmetry in the resulting alkali-metallobismaspheres $[M'@\{(HBi)_{12}M_{20}\}]^{3-}$ and causes the Bi_{12} subcage to shrink (see Tables 2 and Supporting Information S1). This subcage contraction increases from Li_{20}- to Cs_{20}-subshell-containing molecules. Thus, the Bi−Bi distances in the trianionic endohedral frameworks decrease, accompanied by a significant increase of the range of distances. Furthermore, the range of the Bi−M and M−M distances in $[M'@\{(HBi)_{12}M_{20}\}]^{3-}$ is wider in comparison with the ranges in $[(HBi)_{12}M_{20}]^{4-}$. All Bi−Bi distances in $[(HBi)_{12}M_{20}]^{4-}$ and in $[M'@\{(HBi)_{12}M_{20}\}]^{3-}$ structures are longer than the sum of the van der Waals (vdW) radii ($\Delta\Sigma r_{vdW}$ = 480 pm)[6] with exception of those in the trianionic lithium compound (see Supporting Information Table S1). The distances between the bismuth atoms in the Bi_{12} icosahedral subunit increase from the lithium to the cesium structures. The size of the $Bi_{12}M_{20}$ cages also increases from Li_{20} to Cs_{20} subshell-containing tetra-anionic and trianionic cage structures (Table 2). The calculated separations between height and width of the $Bi_{12}M_{20}$ cages in $[M'@\{(HBi)_{12}M_{20}\}]^{3-}$ indicate that the framework becomes more spherical in the case of the heavier alkali-metal homologues (Table 2). The tetra- and trianionic frameworks are nanoscopic cages with around 1 nm diameter.

Similar to the experimental structure[2] of $[Na'@\{(RBi)_{12}Na_{20}\}]^{3-}$ (R = *t*-Bu_3Si), where the Na^+ ion inside the $Bi_{12}Na_{20}$ cage is displaced from the center *Z* (defined as the geometric average of the Bi and alkali-metal atoms in the $Bi_{12}M_{20}$ cage) of the latter by 115.1 pm, the equilibrium structures of the optimized $[M'@\{(HBi)_{12}M_{20}\}]^{3-}$ architectures show strong displacements of the endohedral $M'^{(+)}$ ion: 193.4−233.7 pm for Li_{20} to Cs_{20} subshell-containing molecules (Table 2). According to the VDD atomic charges, the endohedral ion becomes more positive from M′ = Li (+0.25) to Cs (+0.43) (see Table 2). The experimental structure with the diameter of the $Bi_{12}Na_{20}$ cage d_{cage} = 1023.0−929.4 pm (height−width) is more contracted by bulky-ligand effects compared to the one with hydrogen substituents. This factor among the external counterion influences may affect the displacement range of the Na^+ ion inside the $Bi_{12}Na_{20}$ cage.

B. Stability and Reactivity. According to our electron-counting rules for $[(HBi)_{12}M_{20}]^{4-}$ structures, skeletal electron counts for the latter are 72 ($[2(n_{Bi} + n_M) + 8]$ bonding electrons). Hence, with 36 skeletal electron pairs, the shape of $[(HBi)_{12}M_{20}]^{4-}$ corresponds to a closo-spherical architecture $\{[(n_{Bi} + n_M) + 4]$ bonding orbitals, where $(n_{Bi} + n_M) = 32$ for $Bi_{12}M_{20}$ shell$\}$. As a consequence, the compounds should adopt a structure analogous to isoelectronic *closo*-borane $(HB)_{32}^{8-}$.[22]

The reduction of the HOMO−LUMO gap on oligomerization of 10 $HBiM_2$ molecules to $(HBi)_{10}M_{20}$ frameworks indicates an increased reactivity of the latter (see Supporting Information Table S1). The smallest reduction of ca. 0.1 eV is observed for the lithiated double "open-faced" cage, whereas the highest one of ca. 0.7 eV is observed for the sodiated cage. Capping the $(HBi)_{10}M_{20}$ frameworks by two $[HBi]^{2-}$ ions to give $[(HBi)_{12}M_{20}]^{4-}$ results in the most significant reduction of the HOMO−LUMO gap in the case of the lithiated cages (ca. 0.5 eV;

dx.doi.org/10.1021/ic200596c |*Inorg. Chem.* 2011, 50, 5755–5762

Table 2. Calculated Properties of the Tetraanion and Trianion Cage Molecules

		alkali metal (M, M′)				
compound	property	Li	Na	K	Rb	Cs
$(HBi)_{10}M_{20}$	symmetry[a]	D_{5d}	D_{5d}	D_{5d}	D_{5d}	D_{5d}
	d_{cage}[b]	712.5−816.6	807.2−939.0	913.6−1054.4	980.8−1108.4	1030.1−1163.2
	HOMO−LUMO gap[c]	1.58	0.95	0.94	0.76	0.78
	ΔE_1[d]	−442.1	−331.9	−316.0	−288.1	−267.8
$[(HBi)_{12}M_{20}]^{4-}$	symmetry[a,e]	"I_h"	"I_h"	"I_h"	"I_h"	"I_h"
	d_{cage}[b]	922.0−841.7	1035.9−947.1	1146.4−1063.3	1205.2−1124.2	1248.9−1185.4
	HOMO−LUMO gap[c]	1.11	0.82	0.92	0.78	0.75
	ΔE_2[d]	−152.7	−158.9	−154.9	−147.3	−137.3
$[M'@\{(HBi)_{12}M_{20}\}]^{3-}$	d_{cage}[b]	964.5−860.3	1040.0−983.7	1138.9−1088.2	1192.2−1161.2	1236.0−1224.5
	Z−M′[f]	193.4	221.3	229.1	230.2	233.7
	HOMO−LUMO gap[c]	1.15	0.84	0.78	0.63	0.61
	Q(M′)[g]	+0.25	+0.29	+0.39	+0.43	+0.43
	ΔE_3[d]	−259.2	−227.5	−207.4	−202.8	−203.5
	ΔE_{total}[h]	−854.0	−718.3	−678.3	−638.2	−608.6

[a] Symmetry used during the optimization. [b] Diameter of the $Bi_{12}M_{20}$ cage (pm), designated height−width (see Supporting Information Figure S1). [c] HOMO−LUMO gap (eV). [d] Relative energy (including zero-point energy correction) in kcal mol^{-1}. These terms are schematically depicted in Figure 2. [e] The $[(HBi)_{12}M_{20}]^{4-}$ geometries are optimized within D_{5d} symmetry, but possess slightly D_{5d}-distorted I_h symmetry. [f] The distance from the center of the $Bi_{12}M_{20}$ cage (*Z*, defined as the geometric average of the Bi and alkali-metal atoms in the $Bi_{12}M_{20}$ cage) to its endohedral atom M′. [g] The VDD charge (e) on the endohedral atom. [h] The total relative energy (in kcal mol^{-1}) including zero-point energy correction, calculated as $\Delta E_{total} = \Delta E_1 + \Delta E_2 + \Delta E_3$.

see Supporting Information Table S3). The HOMO−LUMO gaps of $[(HBi)_{12}Li_{20}]^{4-}$ and $[Li'@\{(HBi)_{12}Li_{20}\}]^{3-}$ are similar, suggesting that the trapped alkali-metal ion does not contribute much to the kinetic stability of endohedral trianion structures.

The situation is changed if M = K, Rb, Cs in the M_{20}-subshell for the $(HBi)_{12}$ subunits and the same $M'^{(+)}$ (K, Rb, Cs) ions inside of the latter, when the filled trianion cage structures become kinetically less favorable by 0.14 eV than their precursor, tetraanion "empty" ones (Table 2). This means that the endohedral atom in the latter frameworks slightly destabilizes the cage surrounding it. The relatively small values of the HOMO−LUMO gap found for tetraanion and trianion cage molecules are indicative for their low kinetic stability. The larger HOMO−LUMO gaps (see Table 2) that we find for all lithiated compounds suggest that they are kinetically more stable than their heavier alkali-metalated analogues. However, it is also noteworthy that the bulky substituents at Bi like R = *t*-Bu_3Si, used usually to stabilize and protect the bismuth core from external destructive influences, should lead to slightly larger HOMO−LUMO gaps and, as a consequence, higher kinetic stability of the molecules. From this point of view, it seems possible to prepare the lithium-polymetalated systems experimentally, since the sodiated cage structure of $[Na'@\{(RBi)_{12}Na_{20}\}]^{3-}$ with R = *t*-Bu_3Si has been observed.[2]

This scenario is also supported by the relative energies ($\Delta E = \Delta E_1 + \Delta E_2 + \Delta E_3$; see Figure 2) for the studied 5-fold symmetrical molecules. The oligomerization of 10 $HBiM_2$ into the $(HBi)_{10}M_{20}$ framework is an exothermic process with ΔE_1 in the range from −442.1 (M = Li) to −267.8 kcal/mol (M = Cs). Thus, the relative energy of $(HBi)_{10}M_{20}$ is strongly reduced by 174 kcal/mol upon transition from the Li_{20}- to the Cs_{20}-subshell-containing molecules. This trend in ΔE_1 dominates all other trends contained in the terms ΔE_2 and ΔE_3 and is therefore the reason why $(HBi)_{10}Li_{20}$ is the most stable cage. Note that the larger stabilization ΔE_1 in the case of Li also leads to the larger HOMO−LUMO gap mentioned above in connection with a higher kinetic stability for the lithiated systems.

C. Energy Decomposition Analysis (EDA). The EDA for the interactions of ground-state $[(HBi)_{12}M_{20}]^{4-}$ with $M'^{(+)}$ (^1S) in $[M'@\{(HBi)_{12}M_{20}\}]^{3-}$ structures is given in Table 3. Thus, the interaction energies, ΔE_{int}, show the same trend as the dissociation energies, D_e. The difference between these energies is the preparation energy, ΔE_{prep}, which is the energy difference between the equilibrium structures of $[(HBi)_{12}M_{20}]^{4-}$ ions, and the energy of this fragment in the geometry it acquires in the trianionic structures. The calculated D_e values indicate that the interactions between ionic $M'^{(+)}$ and $[(HBi)_{12}M_{20}]^{4-}$ are very strong. The nature of the interactions between the cage's walls and the endohedral alkali-metal ion is predominantly electrostatic (ΔV_{elstat} is around 80% of all bonding interactions $\Delta V_{elstat} + \Delta E_{oi}$). Thus, the electrostatic attraction weakens from Li to Cs and largely determines the trend in overall bond strength.

Macroicosahedral Frameworks: First Principles. On the basis of Wade's electron-counting rules[18a,b] and principles of isolobality[23] and isoelectronicity, we were able to establish the structural and electronic relationships between highly symmetric icosahedral bismuth deltahedra and borane ones as well as the fullerene polyhedra (Scheme 3). The icosahedral decacation *closo*-Bi_{12}^{10+}[20] is isoelectronic to the $(BH)_{12}^{2-}$ dianion (vertices = 12, edges = 30, faces = 20) and dual[24] with a C_{20} dodecahedron (vertices = 20, edges = 30, faces = 12), which is stoichiometrically analogous to Bi_{20}. The ligator-stabilized forms of the family of nonfilled (empty) icosahedral molecules $Bi_n^{(n-2)+}$ are subject to the formula $[(HBi)_nM_{2n-4}]^{4-}$, where n = 12, 32, 92, etc.; i.e., the next members in this series are put forward by the rule for 5-fold symmetrical alkali-metallobismaspheres, $n_{x+1} = 3n_x - 4$, where index x corresponds to the ordinal number of the deltahedron in the icosahedral series with the vertices 12 (x = 1), 32 (x = 2), 92 (x = 3), etc. Index $x + 1$ corresponds to the next member

dx.doi.org/10.1021/ic200596c |*Inorg. Chem.* 2011, 50, 5755–5762

Table 3. Energy Decomposition Analysis (EDA, in kcal/mol) of the Interactions between $[(HBi)_{12}M_{20}]^{4-}$ and $M'^{(+)}$ in $[M'@\{(HBi)_{12}M_{20}\}]^{3-}$ Structures

	M and M′ in $[M'@\{(HBi)_{12}M_{20}\}]^{3-} \rightarrow [(HBi)_{12}M_{20}]^{4-} + M'^{(+)}$				
EDA	Li	Na	K	Rb	Cs
ΔE_{int} [a]	−276.0	−252.1	−228.5	−219.7	−219.7
ΔE_{Pauli}	22.8	21.8	25.6	24.0	23.4
ΔV_{elstat}	−243.8	−220.1	−217.6	−200.0	−198.7
ΔE_{oi}	−55.0	−53.7	−36.4	−43.7	−44.4
ΔE_{prep}	14.0	23.9	20.7	16.7	14.9
D_e [b]	262.0	228.2	207.7	203.0	204.8

[a] $\Delta E_{int} = \Delta V_{elstat} + \Delta E_{Pauli} + \Delta E_{oi}$. [b] $-D_e = \Delta E_{int} + \Delta E_{prep}$.

Scheme 3. Structural and Electronic Relationships between Icosahedral and Macroicosahedral Boron, Carbon, and Bismuth Deltahedral and Polyhedral Molecules[a]

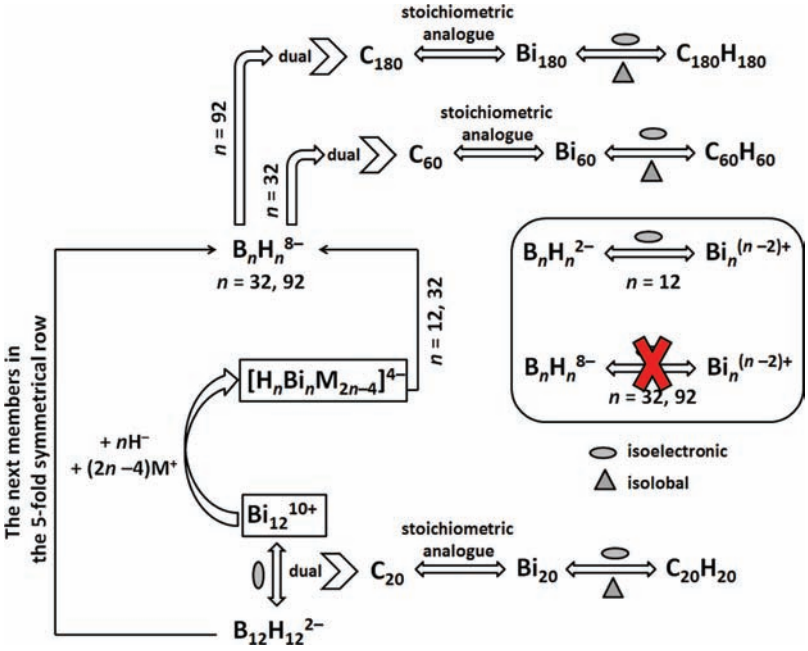

[a] See also ref 25 for a discussion of I_h symmetric allotropes of bismuth, namely, Bi_{20}, Bi_{60}, and Bi_{80}.

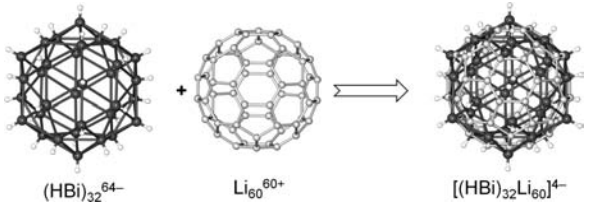

Figure 3. Topological representation of the $[(HBi)_{32}Li_{60}]^{4-}$ salt in which the icosahedral $(HBi)_{32}^{64-}$ subunit is capped by the alkali-metal subshell Li_{60}^{60+} in pentagonal dodecahedral arrangement.

in this icosahedral series 12 (n_1) → 32 (n_2) → 92 (n_3). Thus, the experimentally unknown macroicosahedral deltahedron $[(HBi)_{32}M_{60}]^{4-}$ (Figure 3), isoelectronic to $(HB)_{92}^{8-}$,[22] should be the first possible one after $[(HBi)_{12}M_{20}]^{4-}$ (isoelectronic to $(HB)_{32}^{8-}$)[22] to have a 5-fold symmetry. The rule for the 5-fold symmetrical highly aggregated alkali-metal salts of intermediate "elementanediides" $[RE]^{2-}$ can be expanded to those of the group 15 elements (P, As, Sb). An application of principles of isolobality and isoelectronicity to $[RE]^{2-}$ ions, which are isolobal to X^- halides or O^{2-} oxides, for example, may broaden the above-described concept.

CONCLUSIONS

Bismuth, the heaviest group-15 element, displays a unique tendency to form polyhedral cage molecules, such as the recently discovered, highly aggregated sodium salt of bismuthanediide anions.[2] To assist the further development of synthetic approaches toward this class of compounds, we have computationally analyzed the structure and stability of alkali-metal-supported bismuth polyhedra $[(HBi)_nM_{2n-4}]^{4-}$ as well as the inclusion complexes $[M'@\{(HBi)_nM_{2n-4}\}]^{3-}$ involving an additional endohedral alkali-metal ion $M'^{(+)}$, with n = 12 and M = Li, Na, K, Rb, Cs. We find that the latter are significantly more stable for M = Li than for the heavier alkali metals. Our analyses reveal that this trend is predetermined already by the relative stabilities of

dx.doi.org/10.1021/ic200596c |Inorg. Chem. 2011, 50, 5755–5762

the "open-faced" $[(HBi)_{n-2}M_{2n-4}]$ frameworks. Adding the $[HBi]^{2-}$ caps has relatively little effect on relative stabilities. However, the introduction of the endohedral alkali ions further reinforces the trend that was set by the $[(HBi)_{n-2}M_{2n-4}]$ frameworks. The reason is that endohedral Li^+ enters into a more stabilizing electrostatic interaction with the wall of the cage than the heavier alkali-metal ions. Furthermore, the resulting species also has a relatively large HOMO−LUMO gap which is indicative for enhanced kinetic stability if compared to the heavier alkali-metal homologs. Therefore, our analyses suggest that $[Li'@\{(HBi)_{12}Li_{20}\}]^{3-}$ is the most stable species among the highly aggregated alkali-metals salts of bismuthanediide anions studied herein and may be a viable target for synthesis.

■ ASSOCIATED CONTENT

Supporting Information. Structural data, HOMO−LUMO gaps, and Cartesian coordinates of all stationary points. This material is available free of charge via the Internet at http://pubs.acs.org.

■ AUTHOR INFORMATION

Corresponding Author

*Fax: +49-6221-546617. E-mail: gerald.linti@aci.uni-heidelberg.de (G.L.), F.M.Bickelhaupt@vu.nl (F.M.B).

Present Addresses

[§]Laboratoire de Chimie de Coordination, Institut de Chimie (UMR 7177 CNRS), Université de Strasbourg, 4 Rue Blaise Pascal, F-67081 Strasbourg Cedex, France.

■ ACKNOWLEDGMENT

The work has been performed under the HPC-EUROPA2 project (project number: 228398) with the support of the European Commission—Capacities Area—Research Infrastructures. Further financial support was provided by the National Research School Combination−Catalysis (NRSC-C) and The Netherlands Organization for Scientific Research (NWO-NCF and NWO-CW). K.Y. M. is also grateful to the Graduate College 850 "Molecular Modeling" of the Deutsche Forschungsgemeinschaft (DFG) for providing financial support.

■ REFERENCES

(1) (a) Driess, M. *Acc. Chem. Res.* **1999**, *32*, 1017–1025. (b) Driess, M. *Pure Appl. Chem.* **1999**, *71*, 437–443.

(2) Linti, G.; Köstler, W.; Pritzkow, H. *Eur. J. Inorg. Chem.* **2002**, 2643–2647.

(3) (a) Gouzerh, P.; Proust, A. *Chem. Rev.* **1998**, *98*, 77–111. (b) Müller, A.; Peters, F.; Pope, M. T.; Gatteschi, D. *Chem. Rev.* **1998**, *98*, 239–272.

(4) (a) Cioslowski, J.; Fleischmann, E. D. *J. Chem. Phys.* **1991**, *94*, 3730. (b) Cioslowski, J. *J. Am. Chem. Soc.* **1991**, *113*, 4139. (c) Cioslowski, J.; Lin, Q. *J. Am. Chem. Soc.* **1995**, *117*, 2553. (d) Hu, Y. H.; Ruckenstein, E. *J. Am. Chem. Soc.* **2005**, *127*, 11277.

(5) Mundt, O.; Becker, G.; Rössler, M.; Witthauer, C. *Z. Anorg. Allg. Chem.* **1983**, *506*, 42–58.

(6) Silvestru, C.; Breunig, H. J.; Althaus, H. *Chem. Rev.* **1999**, *99*, 3277–3327.

(7) Hardman, N. J.; Twamley, B.; Power, P. P. *Angew. Chem.* **2000**, *112*, 2884–2886. *Angew. Chem., Int. Ed.* **2000**, *39*, 2771–2773.

(8) Baerends, E. J.; Autschbach, J.; Bérces, A.; Bo, C.; Boerrigter, P. M.; Cavallo, L.; Chong, D. P.; Deng, L.; Dickson, R. M.; Ellis, D. E.; Fan, L.; Fischer, T. H.; Fonseca Guerra, C.; van Gisbergen, S. J. A.; Groeneveld, J. A.; Gritsenko, O. V.; Grüning, M.; Harris, F. E.; van den Hoek, P.; Jacobsen, H.; van Kessel, G.; Kootstra, F.; van Lenthe, E.; McCormack, D. A.; Osinga, V. P.; Patchkovskii, S.; Philipsen, P. H. T.; Post, D.; Pye, C. C.; Ravenek, W.; Ros, P.; Schipper, P. R. T.; Schreckenbach, G.; Snijders, J. G.; Solà, M.; Swart, M.; Swerhone, D.; te Velde, G.; Vernooijs, P.; Versluis, L.; Visser, O.; van Wezenbeek, E.; Wiesenekker, G.; Wolff, S. K.; Woo, T. K.; Ziegler, T. *ADF2010.01*; SCM, Theoretical Chemistry, Vrije Universiteit, Amsterdam, The Netherlands, http://www.scm.com.

(9) (a) te Velde, G.; Bickelhaupt, F. M.; Baerends, E. J.; Fonseca Guerra, C.; van Gisbergen, S. J. A.; Snijders, J. G.; Ziegler, T. *J. Comput. Chem.* **2001**, *22*, 931–967.(b) Fonseca Guerra, C.; Visser, O.; Snijders, J. G.; te Velde, G.; Baerends, E. J. In *Methods and Techniques for Computational Chemistry*; Clementi, E., Corongiu, G., Eds.; STEF: Cagliari, 1995; pp 305−395. (c) Baerends, E. J.; Ellis, D. E.; Ros, P. *Chem. Phys.* **1973**, *2*, 41–51. (d) Baerends, E. J.; Ros, P. *Chem. Phys.* **1975**, *8*, 412–418. (e) Baerends, E. J.; Ros, P. *Int. J. Quantum Chem. Symp.* **1978**, *12*, 169–190. (f) Fonseca Guerra, C.; Snijders, J. G.; te Velde, G.; Baerends, E. J. *Theor. Chem. Acc.* **1998**, *99*, 391–403. (g) Boerrigter, P. M.; te Velde, G.; Baerends, E. J. *Int. J. Quantum Chem.* **1988**, *33*, 87–113. (h) te Velde, G.; Baerends, E. J. *J. Comput. Phys.* **1992**, *99*, 84–98. (i) Snijders, J. G.; Vernooijs, P.; Baerends, E. J. *At. Data Nucl. Data Tables* **1981**, *26*, 483–509.(j) Krijn, J.; Baerends, E. J. *Fit-Functions in the HFS-Method; Internal Report (in Dutch)*; Vrije Universiteit: Amsterdam, 1984. (k) Versluis, L.; Ziegler, T. *J. Chem. Phys.* **1988**, *88*, 322–328.(l) Slater, J. C. *Quantum Theory of Molecules and Solids*; McGraw-Hill: New York, 1974; Vol. 4. (m) Becke, A. D. *J. Chem. Phys.* **1986**, *84*, 4524–4529. (n) Becke, A. D. *Phys. Rev. A* **1988**, *38*, 3098–3100. (o) Vosko, S. H.; Wilk, L.; Nusair, M. *Can. J. Phys.* **1980**, *58*, 1200–1211. (p) Perdew, J. P. *Phys. Rev. B* **1986**, *33*, 8822–8824.(Erratum: *Phys. Rev. B* **1986**, *34*, 7406). (q) Fan, L.; Ziegler, T. *J. Chem. Phys.* **1991**, *94*, 6057–6063.

(10) (a) Bérces, A.; Dickson, R. M.; Fan, L.; Jacobsen, H.; Swerhone, D.; Ziegler, T. *Comput. Phys. Commun.* **1997**, *100*, 247–262. (b) Jacobsen, H.; Bérces, A.; Swerhone, D.; Ziegler, T. *Comput. Phys. Commun.* **1997**, *100*, 263–276. (c) Wolff, S. K. *Int. J. Quantum Chem.* **2005**, *104*, 645–659.

(11) van Lenthe, E.; Baerends, E. J.; Snijders, J. G. *J. Chem. Phys.* **1994**, *101*, 9783–9792.

(12) (a) Bickelhaupt, F. M.; Baerends, E. J. In *Reviews in Computational Chemistry*; Lipkowitz, K. B., Boyd, D. B., Eds.; Wiley-VCH: New York, 2000; Vol. 15, p 1. (b) Bickelhaupt, F. M.; Nibbering, N. M. M.; van Wezenbeek, E. M.; Baerends, E. J. *J. Phys. Chem.* **1992**, *96*, 4864. (c) Bickelhaupt, F. M.; Diefenbach, A.; de Visser, S. P.; de Koning, L. J.; Nibbering, N. M. M. *J. Phys. Chem. A* **1998**, *102*, 9549–9553.

(13) (a) Ziegler, T.; Rauk, A. *Theor. Chim. Acta* **1977**, *46*, 1. (b) Ziegler, T.; Rauk, A. *Inorg. Chem.* **1979**, *18*, 1558. (c) Ziegler, T.; Rauk, A. *Inorg. Chem.* **1979**, *18*, 1755.

(14) (a) See also:Kitaura, K.; Morokuma, K. *Int. J. Quantum Chem.* **1976**, *10*, 325. (b) Morokuma, K. *Acc. Chem. Res.* **1977**, *10*, 294.

(15) Baerends, E. J.; Gritsenko, O. V. *J. Phys. Chem. A* **1997**, *101*, 5383.

(16) (a) Bickelhaupt, F. M.; van Eikema Hommes, N. J. R.; Fonseca Guerra, C.; Baerends, E. J. *Organometallics* **1996**, *15*, 2923. See also: (b) Fonseca Guerra, C.; Handgraaf, J.-W.; Baerends, E. J.; Bickelhaupt, F. M. *J. Comput. Chem.* **2004**, *25*, 189–210. Voronoi cells are equivalent to Wigner−Seitz cells in crystals; for the latter, see:(c) Kittel, C. *Introduction to Solid State Physics*; Wiley: New York, 1986.

(17) Hirshfeld, F. L. *Theor. Chim. Acta* **1977**, *44*, 129.

(18) (a) Wade, K. *Chem. Commun.* **1971**, 792. (b) Wade, K. *Adv. Inorg. Chem. Radiochem.* **1976**, *18*, 1. (c) Williams, R. E. *Inorg. Chem.* **1971**, *10*, 210. (d) Williams, R. E. *Adv. Inorg. Chem. Radiochem.* **1976**, *18*, 67. (e) Rudolph, R. W.; Pretzer, W. R. *Inorg. Chem.* **1972**, *11*, 1974. (f) Rudolph, R. W. *Acc. Chem. Res.* **1976**, *9*, 446.

(19) (a) Hershaft, A.; Corbett, J. D. *Inorg. Chem.* **1963**, *2*, 979. (b) Ulvenlund, S.; Stahl, K.; Bengtsson-Kloo, L. *Inorg. Chem.* **1996**, *35*, 223. (c) Beck, J.; Brendel, C. J.; Bengtsson-Kloo, L.; Krebs, B.; Mummert, M.; Stankowski, A.; Ulvenlund, S. *Chem. Ber* **1996**, *129*, 1219.

(d) Ruck, M. *Z. Anorg. Allg. Chem.* **1998**, *624*, 521. (e) Ruck, M.; Dubensky, V.; Söhnel, T. *Angew. Chem., Int. Ed.* **2003**, *42*, 2978. (f) Wahl, B.; Ruck, M. *Z. Anorg. Allg. Chem.* **2009**, *636*, 337.

(20) (a) Kuznetsov, A. N.; Kloo, L.; Lindsjö, M.; Rosdahl, J.; Stoll, H. *Chem.—Eur. J.* **2001**, *7*, 2821–2828.(b) Bi_{12}^{10+} should adopt a structure with the global minimum symmetry I_h according to Wade's rules. In their computations, Kuznetsov et al. have used the small and large core ECP to optimize *closo*-Bi_{12}^{10+}. However, they have not been able to identify a true local minimum for the latter.

(21) Monakhov, K. Yu.; Zessin, T.; Linti, G. *Eur. J. Inorg. Chem.* **2010**, 3212–3219.

(22) Wang, Z.-X.; Schleyer, P. v. R. *J. Am. Chem. Soc.* **2003**, *125*, 10484–10485.

(23) Hoffmann, R. *Angew. Chem.* **1982**, *94*, 752.*Angew. Chem., Int. Ed.* **1982**, *21*, 711.

(24) (a) Chen, Z.; King, R. B. *Chem. Rev.* **2005**, *105*, 3613–3642. (b) Polyhedra are dual if the number of vertices of one polyhedron corresponds to the number of faces of another and vice versa.

(25) Zdetsis, A. D. *J. Phys. Chem. C* **2010**, *114*, 10775–10781.